

Experimental evidence for magnetorotational instability in a helical magnetic field

Frank Stefani, Thomas Gundrum, Gunter Gerbeth
 Forschungszentrum Rossendorf, P.O. Box 510119, D-01314 Dresden, Germany

Günther Rüdiger, Manfred Schultz, Jacek Szklarski
 Astrophysikalisches Institut Potsdam, An der Sternwarte 16, D-14482 Potsdam, Germany

Rainer Hollerbach
 Department of Applied Mathematics, University of Leeds, Leeds, LS2 9JT, United Kingdom

A recent paper [R. Hollerbach and G. Rüdiger, Phys. Rev. Lett. **95**, 124501 (2005)] has shown that the threshold for the onset of the magnetorotational instability (MRI) in a Taylor-Couette flow is dramatically reduced if both axial and azimuthal magnetic fields are imposed. In agreement with this prediction, we present results of a Taylor-Couette experiment with the liquid metal alloy GaInSn, showing evidence for the existence of the MRI at Reynolds numbers of order 1000 and Hartmann numbers of order 10.

The role of magnetic fields in the cosmos is two-fold: First, planetary, stellar and galactic fields are a product of the homogeneous dynamo effect in electrically conducting fluids. Second, magnetic fields are also believed to play an active role in cosmic structure formation, by enabling outward transport of angular momentum in accretion disks via the magnetorotational instability (MRI) [1]. Considerable theoretical and computational progress has been made in understanding both processes. The dynamo effect has even been verified experimentally, in large-scale liquid sodium facilities in Riga and Karlsruhe, and continues to be studied in laboratories around the world [2]. In contrast, obtaining the MRI experimentally has been less successful thus far [3]. ([4] claim to have observed it, but their background state was already fully turbulent, thereby defeating the original idea that the MRI would destabilize an otherwise stable flow.)

If only an axial magnetic field is externally applied, the azimuthal field that is necessary for the occurrence of the MRI must be produced by induction effects, which are proportional to the magnetic Reynolds number (Rm) of the flow. But why not substitute this induction process simply by *externally applying an azimuthal magnetic field as well?* This question was at the heart of the paper [5], where it was shown that the MRI is then possible with far smaller Reynolds (Re) and Hartmann (Ha) numbers. In this paper we report experimental verification of this idea, presenting evidence of the MRI in a liquid metal Taylor-Couette (TC) flow with externally imposed axial and azimuthal (i.e., helical) magnetic fields.

The heart of our facility ‘PROMISE’ (Potsdam ROssendorf Magnetic InStability Experiment) is a cylindrical vessel made of copper (see Fig. 1). The use of copper was motivated by the fact that the instability usually occurs at lower Reynolds and Hartmann numbers for the case of ideally conducting boundaries than for non-conducting boundaries [6]. The inner wall is 10 mm thick, and extends in radius from 22 to 32 mm; the outer wall is 15 mm thick, extending from 80 to 95 mm in r .

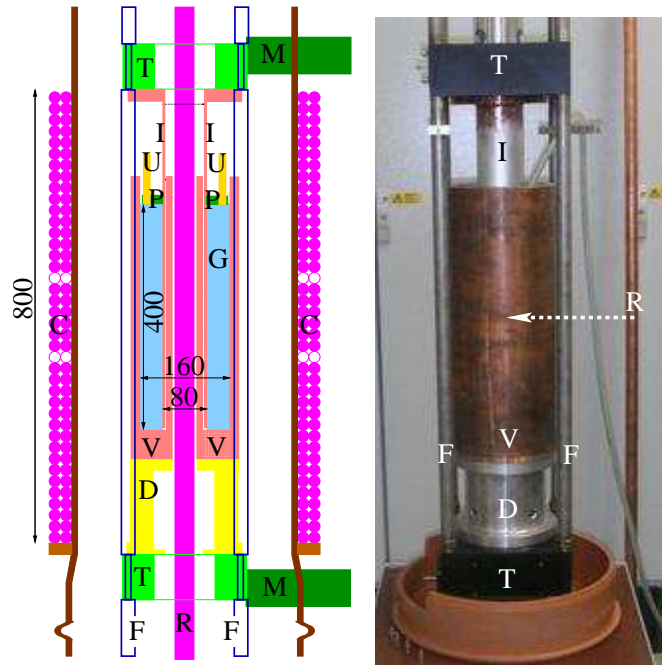


FIG. 1: Sketch (left) and photograph (right) of the central module of the PROMISE facility. V - Copper vessel, I - Inner cylinder, G - GaInSn, U - Two ultrasonic transducers, P - Plexiglass lid, T - High precision turntables, M - Motors, F - Frame, C - Coil, R - Central rod. The dimensions are in mm. When the experiment is running, the rod R in the right picture goes through the center of the cylinders.

This vessel is filled with the alloy $\text{Ga}^{67}\text{In}^{20.5}\text{Sn}^{12.5}$, which is liquid at room temperatures. The physical properties of GaInSn at 25 °C are: density $\rho = 6.36 \times 10^3 \text{ kg/m}^3$, kinematic viscosity $\nu = 3.40 \times 10^{-7} \text{ m}^2/\text{s}$, electrical conductivity $\sigma = 3.27 \times 10^6 \text{ }(\Omega \text{ m})^{-1}$. The magnetic Prandtl number is then $Pm = \mu_0 \sigma \nu = 1.40 \times 10^{-6}$.

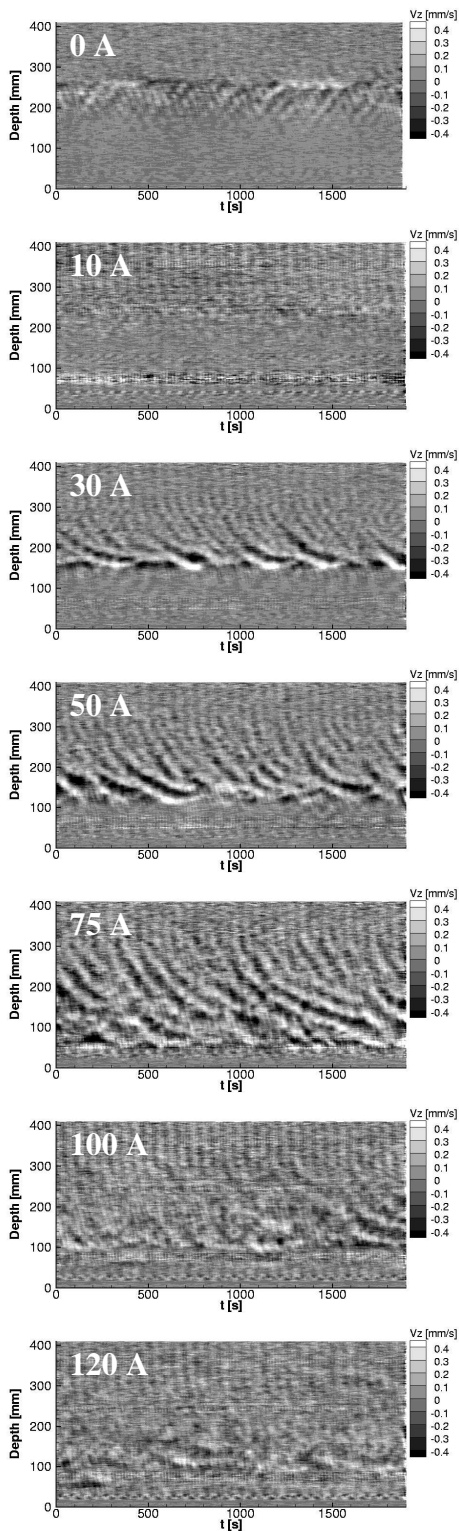


FIG. 2: Measured axial velocity in dependence on time and depth for different coil currents.

The copper vessel is fixed, via an aluminum spacer D,

on a precision turntable T; the outer wall of the vessel thus serves as the outer cylinder of the TC flow. The inner cylinder of the TC flow is fixed to an upper turntable, and is immersed into the GaInSn from above. It has a thickness of 4 mm, extending in radius from 36 to 40 mm. There is thus a gap of 4 mm between this immersed cylinder and the inner wall of the containment vessel. The actual TC flow then extends between $r_{in} = 40$ mm and $r_{out} = 80$ mm. At the moment, the upper endplate is a plexiglass lid P fixed to the frame F. In contrast, the bottom is simply part of the copper vessel, and hence rotates with the outer cylinder. There is thus a clear asymmetry in the endplates, with respect to both their rotation rates and electrical conductivities.

Note also that the accuracy of this setup is not quite at the $\sim 10^{-2}$ mm level that can be achieved in ordinary, hydrodynamic TC experiments, e.g. [7]. For example, in order to ensure a well-defined electrical contact between the GaInSn and the walls, it is necessary to intensively rub the fluid into the copper. The precision is then more like 10^{-1} mm. The Reynolds number $Re = 2\pi f_{in} r_{in} (r_{out} - r_{in}) / \nu$ is also $O(10^3)$, considerably greater than the $Re_c = 68$ value obtained in the nonmagnetic problem (with stationary outer cylinder).

Axial magnetic fields of order 10 mT are produced by a double-layer coil (C). The omission of windings at two symmetric positions close to the middle resulted from a coil optimization to maximize the homogeneity of the axial field throughout the volume occupied by the liquid. This coil is fed by a power supply that can deliver up to 200 A. The azimuthal field, also of order 10 mT, is generated by a current through a water-cooled copper rod R of radius 15 mm. The power supply for this axial current delivers up to 8000 A.

At present, the measuring instrumentation consists exclusively of two ultrasonic transducers with a working frequency of 4 MHz; these are fixed into the plexiglass lid, 15 mm away from the outer copper walls, flash mounted at the interface to the GaInSn. They provide full axial velocity profiles along the ultrasound beamline by means of Ultrasound Doppler Velocimetry (UDV) [8]. A similar measuring system for the axial velocity components in TC experiments was first described by Takeda [9]. The comparison of the two signals from two opposite sensors is important in order to clearly distinguish between the expected axisymmetric ($m = 0$) MRI mode [6] and certain $m = 1$ modes which also play a role in some parameter regions of the experiment.

Typically, the duration of the experimental runs was 1900 sec, after a waiting time of one hour. Such a long waiting time was chosen not only due to the hydrodynamic gap diffusion time, but also due to our numerical predictions of rather small growth rates of the MRI mode in helical fields (see also [10]).

One of the features of TC flow under the influence of helical magnetic fields is the replacement of the Taylor

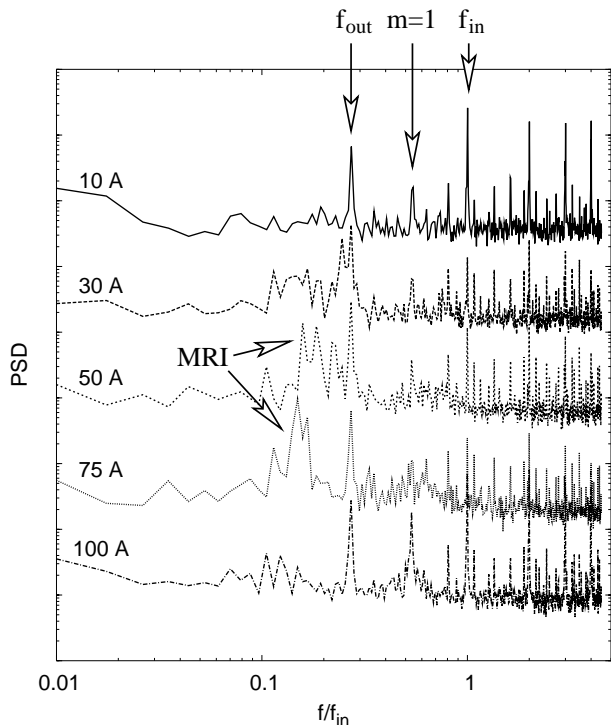


FIG. 3: Power spectra of the v_z fluctuations, averaged over the depths between 220 and 308 mm, for 5 different coil currents. The frequencies of the inner and outer cylinder are indicated. The MRI is visible at 50 and 75 A. In addition to that, an $m = 1$ mode is also present.

vortex flow by a travelling wave [5, 6]. This travelling wave appears already at $\mu := f_{\text{out}}/f_{\text{in}} = 0$, although with a very low frequency. With increasing μ , the frequency increases and typically reaches a value of $0.2f_{\text{in}}$ at the Rayleigh line $\mu_{\text{Ray}} = (r_{\text{in}}/r_{\text{out}})^2 =: \eta^2$ (we have $\eta = 0.5$ here, hence $\mu_{\text{Ray}} = 0.25$). The crucial point now is that under the influence of helical magnetic fields, the critical Reynolds numbers remain relatively small increasingly far beyond the Rayleigh line, where nothing special happens. Typically, this shift to larger μ becomes larger for increasing values of the ratio $\beta := B_{\varphi}(r = r_{\text{in}})/B_z$ of azimuthal field to axial field.

Another typical feature of the MRI is that, for fixed Re , it sets in at a certain critical value of the Hartmann number $Ha = B_z(r_{\text{in}}(r_{\text{out}} - r_{\text{in}})\sigma/\rho\nu)^{1/2}$, and disappears again at some higher value. In this letter we focus exclusively on experimental results which substantiate this behavior.

All results presented in the following are for rotation rates of $f_{\text{in}} = 0.06 \text{ s}^{-1}$ and $f_{\text{out}} = 0.0162 \text{ s}^{-1}$, i.e. for $\mu = 0.27$, beyond the Rayleigh line $\mu_{\text{Ray}} = 0.25$. Figure 2 documents a selection of seven experimental runs for coil currents I_{coil} between 0 and 120 A. In each case, the axial current I_{rod} was fixed to 6000 A. The color coding

of the plots indicates the (negative) axial velocity component measured along the ultrasound beam, from which we have subtracted the depth-dependent time average in order to filter out the two Ekman vortices which appear already without any magnetic field. These vortices, characterized by inward radial flows close to the upper and lower endplates, show up in our UDV data in the form of positive and negative axial velocities, separated approximately at mid-height by a rather sharp boundary. This boundary most likely corresponds to a jet-like radial outflow in the center of the cylinder, as discussed in [11].

For $I_{\text{coil}} = 30 \text{ A}$ we already observe a traveling wave-like structure which is, however, still restricted to the middle part of the cylinder. One might speculate that, due to the (jet-like) radial outward flow there, fluid with lower angular momentum is transported outward, which leads to a steeper decrease of v_{φ} and hence to a (locally) lower value μ than what would be expected from the rotation ratio of outer to inner cylinder [11].

For increasing I_{coil} , this traveling wave becomes more and more dominant, until at 75 A it fills essentially the entire cylinder. Increasing I_{coil} even further though, at 100 A this wave ceases to exist, and we again have a rather featureless flow. This is shown more quantitatively in Fig. 3, where we show the average over the depths 220-308 mm of the power spectral density for the axial velocity for 5 selected values of I_{coil} . A feature common to all five curves is the appearance of the rotation rates of the inner and outer cylinders. This reflects certain geometric imperfections of the facility, probably in the form of cylinder eccentricities or metal oxides sticking to some parts of the walls. There is also a certain peak approximately at the mean of the inner and outer cylinder frequencies, which, on closer inspection of the two transducer signals, turns out to be a non-axisymmetric $m = 1$ mode. Most interesting for us here, however, is the MRI mode at $f/f_{\text{in}} \sim 0.1 - 0.2$. These frequencies have been analyzed in detail for all values of I_{coil} chosen in the experiment.

We now interpret these experimental data in the context of numerical predictions, obtained and cross-checked by various independent codes [5, 12, 13] for the solution of the linear eigenvalue problem in unbounded cylinders. First, Fig. 4a shows the dependence of the critical Reynolds number on the Hartmann number. We observe the typical MRI behavior, with the minimum value of Re_{crit} occurring at $Ha = 7.7$. Fig. 4b compares the measured frequencies of the travelling wave, normalized to the rotation rate of the inner cylinder, with the computed ones. The latter are actually given in two versions, at Re_{crit} , and at the experimental value $Re = 1775$. It is interesting that the difference between the two curves is relatively small. Hence it might be anticipated that the normalized frequency in the nonlinear (saturated) regime is probably also not far from these values. The measured frequencies are in reasonable correspondence with

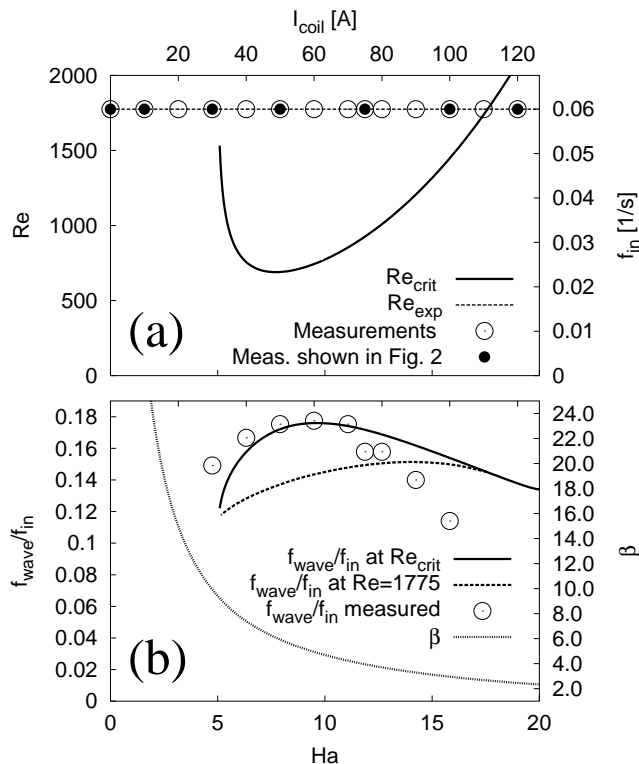


FIG. 4: (a) Computed critical Reynolds numbers for varying I_{coil} (and hence Hartmann numbers), for fixed $I_{rod} = 6000$ A. (b) Frequency f_{wave} of the travelling MRI wave, normalized to the rotation rate f_{in} of the inner cylinder. The ratio of azimuthal field to axial field β is also shown.

the computed ones, and show a similar behavior, with a maximum close to $Ha = 10$.

In summary, we have provided experimental evidence for the existence of the MRI in current-free helical magnetic fields, by showing its appearance in a certain interval of Hartmann numbers, in reasonable agreement with numerical predictions. Further experimental results for other combinations of the governing parameters will be published elsewhere. Certainly, much work remains to be done, including a detailed investigation into the role

of the magnetic axial boundary conditions. For later experiments, a symmetrization of these boundaries is envisioned. Connected with this, a suppression of the Ekman vortices by means of split rings (proposed in [11], see also [14]) may also help to avoid special effects in the mid-height of the cylinder.

This work was supported by the German Leibniz Gemeinschaft, within its SAW program. We thank R. Rosner for his interest and support for this work, Heiko Kunath for technical assistance, and Markus Meyer for assistance taking some of the data. The Rossendorf group also thanks Janis Priede and Ilmars Grants for stimulating discussions.

-
- [1] S.A. Balbus and J. F. Hawley, *Astrophys. J.* **376**, 214 (1991).
 - [2] A. Gailitis, O. Lielausis, E. Platacis, G. Gerbeth, and F. Stefani, *Rev. Mod. Phys.* **74**, 973 (2002).
 - [3] *MHD Couette Flows: Experiments and Models*, edited by R. Rosner, G. Rüdiger, and A. Bonanno, AIP Conf. Proc. No. 733 (AIP, New York, 2004).
 - [4] D.R. Sisan, N. Mujica, W.A. Tillotson, Y.M. Huang, W. Dorland, A.B. Hassam, T.M. Antonsen, and D.P. Lathrop, *Phys. Rev. Lett.* **93**, 114502 (2004).
 - [5] R. Hollerbach and G. Rüdiger, *Phys. Rev. Lett.* **95**, 124501 (2005).
 - [6] G. Rüdiger, R. Hollerbach, M. Schultz, and D.A. Shalybkov, *Astron. Nachr.* **326**, 409 (2005).
 - [7] F. Schultz-Grunow, *Z. Angew. Math. Mech.* **39**, 101 (1959).
 - [8] A. Cramer, C. Zhang, and S. Eckert, *Flow Meas. Instrum.* **15**, 145 (2004).
 - [9] Y. Takeda, W.E. Fischer, J. Sakakibara, and K. Ohmura, *Phys. Rev. E* **47**, 4130 (1993).
 - [10] W. Liu, J. Goodman, I. Herron, and H. Ji, *astro-ph/0606125* (2006).
 - [11] A. Kageyama, H. Ji, J. Goodman, F. Chen, and E. Shoshan, *J. Phys. Soc. Jpn.* **73**, 2424 (2004).
 - [12] G. Rüdiger, M. Schultz, and D. Shalybkov, *Phys. Rev. E* **67**, 046312 (2003).
 - [13] F. Stefani and G. Gerbeth, In [3], p. 100.
 - [14] R. Hollerbach and A. Fournier, In [3], p. 114.